RSC Advances




ROYAL SOCIETY OF CHEMISTRY

www.rsc.org/advances

RSC Advances

RSCPublishing

ARTICLE

# Cs Promoted $Fe_5C_2$/Charcoal Nanocatalysts for Sustainable Liquid Fuel Production

Cite this: DOI: 10.1039/x0xx00000x

Ji Chan Park,[a,b,]* Dong Hyun Chun,[a,b] Jung-Il Yang,[a] Ho-Tae Lee,[a] Sungjun Hong,[a] Geun Bae Rhim,[a] Sanha Jang [a] and Heon Jung[a]*

Received 00th January 2012,
Accepted 00th January 2012

DOI: 10.1039/x0xx00000x

www.rsc.org/

Cs promoted $Fe_5C_2$/charcoal nanocatalysts bearing small iron carbide particles of 8.5 and 14 nm were prepared through a simple melt-infiltration process and a wetness impregnation method; resulting materials showed very high CO conversion (>95%) and good selectivity, especially at Cs/Fe=0.025, resulting in a high liquid oil productivity (~0.4 $g_{liq}•g_{cat}^{-1}•h^{-1}$) in high-temperature Fischer-Tropsch synthesis.

## Introduction

Fischer-Tropsch (FT) synthesis is known as an effective method to convert mixtures of CO and $H_2$ gasses produced from fossil resources such as coal and natural gas to liquid fuels.[1-3] In the FT reaction, the hydrocarbon products, normally obtained in the presence of cobalt- and iron-based catalysts, are distributed into gaseous hydrocarbons ($C_1$-$C_4$), liquid oil, and solid wax.[4-6] Recently, lower-olefins as key building blocks of chemicals have been selectively synthesized by FTO (Fischer-Tropsch to Olefins) process using Fe/α-$Al_2O_3$ or Fe/CNF (carbon-nanofiber) catalysts promoted by Na and S under low reaction pressure (~1 bar).[7-9] However, the hydrogenation of CO under lowered pressure of feed gas exhibited a much lower CO conversion of ~1% compared to the value of 70~80% obtainable under elevated pressure (15~20 bar). In order to obtain liquid hydrocarbons with higher productivity using an Fe-based catalyst, FT synthesis still should be run under elevated reaction pressure. On the other hand, the hydrocarbon product distribution has been effectively controlled by changing the catalyst type and reaction conditions for further applications such as transportation and chemicals.[10-13] For example, it has been possible to obtain gasoline-range hydrocarbons more selectively by using bi-functional catalysts of the Co- and Fe-zeolite hybrid system.[14-16] A micro-porous aluminosilicate material like ZSM-5 as an acid catalyst has been found to enhance the hydrocarbon product selectivity, but, because of its limited surface area with small pore volume and size, has normally led to decreased catalyst activity, especially in cases of high metal load.

In FT synthesis, an Fe-based catalyst has a big advantage applicable to wide range $H_2$/CO feed ratios (0.5~2.5) owing to its water-gas-shift (WGS) reaction activity,[17-18] which makes the catalyst widely used for various gas types, such as those derived from biomass- or coal-gasification. In particular, high-temperature FT synthesis, normally operated at temperatures of 300-350 °C in the presence of an Fe-based catalyst, can more strongly shift the hydrocarbon product selectivity from long carbon chains to short ones.[19] Although the cheaper Fe catalyst has been known to be less active than the much more expensive Co catalyst (Co price is approximately 200 times the price of Fe) under similar reaction temperature conditions (200-240 °C), the elevated reaction temperature conditions (>300 °C) can make the activity of an Fe-based catalyst much higher due to the enhanced mass transfer and reaction speed.

In terms of the catalyst activity, formation of Hägg-carbide ($Fe_5C_2$) species by controlling the activation process using CO or mixed gas was crucial.[20-22] For the catalyst preparation, a few colloidal methods for the synthesis of active and uniform $Fe_5C_2$ nanoparticles have been reported,[23-24] but still had problems in the scale-up process due to the high price of the metal precursors and solvents, as well as the complicated preparation method. Recently, a melt-infiltration method without use of any solvent has been found to be an effective way to prepare uniform supported catalysts such as Co/SBA-15 and Pd/C with enhanced metal dispersion and distribution.[25-27] Among the various support materials (e.g., $Al_2O_3$, $SiO_2$, MgO, activated carbon), an activated charcoal made of wood can be a good carbon-based support; this material is commercially applicable because of its low cost, thermal stability, high surface area (~1000 $m^2•g^{-1}$), and large pore volume (~0.8 $cm^3•g^{-1}$).

Alkali and alkali-earth metals (e. g., Na, K, Ca) as base promoters donating electrons to active surfaces have led to the enhanced performance of Fe-based catalysts in terms of activity and selectivity.[28-30] For instance, the addition of a small amount of K greatly enhanced the activity and selectivity of the Fe-based catalyst by facilitating CO dissociation and increasing the carbon-chain growth on the catalyst surface.[31] The effect of K as a base promoter has been studied extensively,[32] but fewer studies have dealt with the positive effect of Cs, which has been found to have a higher basicity than those of Na, K and Rb, thus far.[33] The catalyst carburization and olefin selectivity were also correlated to the basicity of the promoter in the order Cs > Rb > K > Na > unpromoted.[28,34] In particular, although a few studies on effects of Cs on Fe and Co catalysts have been attempted, the effect for Cs contents especially in the Hägg-carbide structure has not been clearly reported in experiment. In the present work, we report a facile synthetic method for active and selective Cs promoted $Fe_5C_2$ nanoparticles via melt-infiltration and a wetness impregnation process that exploits a porous charcoal support. The Cs promoted $Fe_5C_2$/charcoal catalysts show very high activity and liquid productivity as well

**Scheme 1.** Synthetic scheme of Cs promoted $Fe_5C_2$/charcoal catalyst.

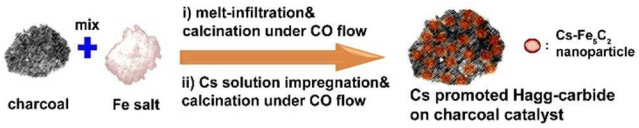


as good stability without deactivation for 90 h in high-temperature FT reaction conditions under 320 °C at 15 bar.

## Experimental

**Preparation of Cs promoted $Fe_5C_2$/charcoal catalyst:** 4.6 mmol of $Fe(NO_3)_3$•$9H_2O$ (Sigma-Aldrich, ACS reagent, ≥98%) was physically ground with 1.0 g of activated charcoal (Sigma-Aldrich, −100 mesh particle size) in a mortar for several minutes under ambient conditions until the powder was homogeneously black. After grinding, the resulting powder was placed in a polypropylene bottle and aged at 323 K in an oven. After aging for 24 h, the cooled sample, now at room temperature, was transferred to an alumina boat in a tube-type furnace. Finally, the iron-incorporated charcoal powder was slowly heated at a ramping rate of 2.7 K•$min^{-1}$ to 623 K under a CO flow of 200 mL•$min^{-1}$; it was then thermally treated at 623 K for 4h under a continuous CO flow. After thermal treatment, the resulting black powder was cooled to room temperature, and then submerged into 20 mL of anhydrous ethanol under an $N_2$ flow of 500 mL•$min^{-1}$. The immersed Fe/C powder was simply separated using a magnet and completely dried in a vacuum oven at 323 K. $Cs_2CO_3$ (Aldrich, ReagentPlus, 99%) dissolved in distilled water was impregnated on the dried Fe/C powder by incipient wetness method.[35] The 0.023 mmol, 0.057 mmol, 0.114 mmol, and 0.228 mmol of $Cs_2CO_3$ salt were used for the preparation of Cs promoted $Fe_5C_2$ catalysts at Cs/Fe=0.010, Cs/Fe=0.025, Cs/Fe=0.050, and Cs/Fe=0.100, respectively. The Cs-incorporated sample was thermally treated again at 623 K for 4h under a continuous CO flow of 200 mL•$min^{-1}$. Then, the resulting powder was cooled to room temperature and submerged again in anhydrous ethanol under $N_2$ flow. Finally, the powder was separated and dried in a vacuum oven at 323 K.

**Fischer-Tropsch synthesis:** Fischer-Tropsch (FT) reactions were carried out in a fixed-bed stainless steel reactor with inner diameter of 5 mm and length of 180 mm. The catalyst (0.3g) was diluted with glass beads (3.5 g, 425~600 μm size) for prevention of hot-spot generation and then placed in the fixed-bed reactor. The catalyst was reactivated in-situ under a CO flow of 40 mL•$min^{-1}$ at 623 K for 4 h. Then, the reaction was performed at 320°C and 15 bar for 90 h using synthesis gas ($H_2$/CO = 1.0, GHSV=8.0 NL•$g_{cat}^{-1}$•$h^{-1}$). The flow rates of the outlet gasses were measured by a wet-gas flow meter (Shinagawa Co.); gasses were analysed using an online gas chromatograph (Agilent, 3000A Micro-GC) equipped with molecular sieve and plot Q columns. After the 90 h of Fischer-Tropsch synthesis, the solid hydrocarbon products were collected in a hot trap at 503 K and the liquid hydrocarbon products and water were collected in a cold trap at 273 K. The composition of wax and liquid oil was analysed by means of an offline GC (Agilent, 6890 N) with a simulated distillation method (ASTM D2887).

**Characterization:** The obtained samples were characterized using an HRTEM (Tecnai G2 F30 operated at 300 kV, KAIST).

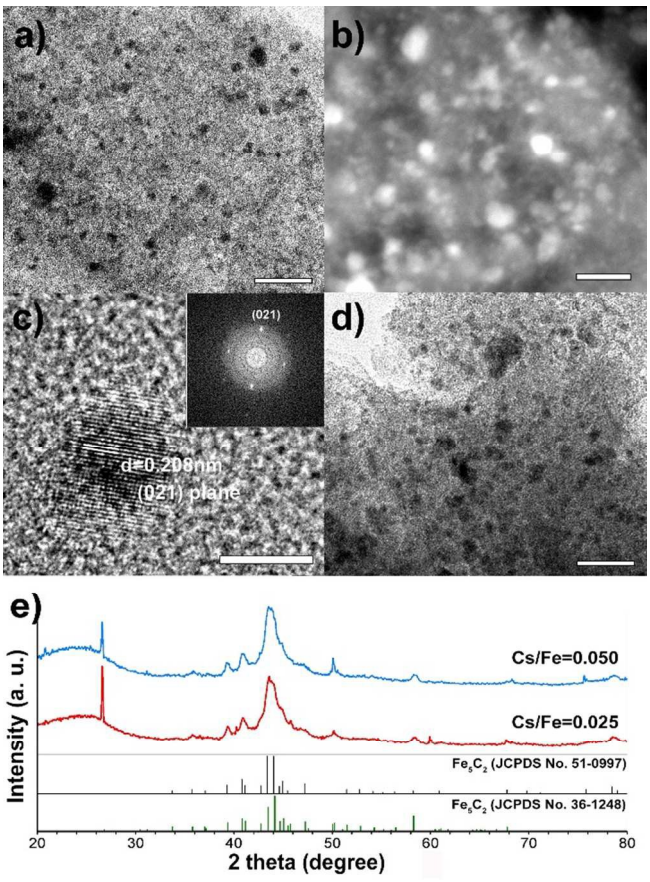


**Fig. 1.** (a) TEM and (b) HADDF-STEM images of Cs promoted $Fe_5C_2$/charcoal at Cs/Fe = 0.025, (c) HRTEM image of the Cs promoted $Fe_5C_2$ single particle with corresponding FT pattern (inset of c), (d) TEM image of Cs promoted $Fe_5C_2$/charcoal at Cs/Fe=0.050, and (e) XRD spectra of Cs promoted $Fe_5C_2$/charcoal catalysts. The bars represent 50 nm (a,d), 20 nm (b), and 5 nm (c).

For TEM analysis, samples were prepared by putting a few drops of the corresponding colloidal solutions on formvar-carbon copper grids (Ted Pellar, Inc). High power powder-XRD (Rigaku D/MAX-2500, 18kW) was also used for analysis. X-ray photoelectron spectroscopy (XPS) study was carried out using a Thermo VG Multilab 2000 spectrometer with a monochromatic Al Kα source. $N_2$ sorption isotherms were measured at 77 K with a TriStar II 3020 surface area analyser. Before measurement, the samples were degassed in a vacuum at 573 K for 4 h. The surface basicity of the catalysts was analysed by temperature-programmed desorption (TPD) using $CO_2$ as an adsorbent. The catalysts (about 0.1g) were purged with a He flow of 30 mL•$min^{-1}$ at 423 K for 2 h to remove the adsorption species from the catalyst surface. After cooling the catalysts to 323 K, $CO_2$ was introduced into the sample cell for 30 min and this was followed by purging with He for 30 min to remove weakly adsorbed species. After that, the catalyst sample was heated again to 673 K at a heating rate of 10 K• $min^{-1}$ in a He flow of 15 mL•$min^{-1}$ and the temperature was then held at the maximum temperature for 20 min. The amount of $CO_2$ desorption was measured by a thermal conductivity detector (TCD).

## Results and discussion

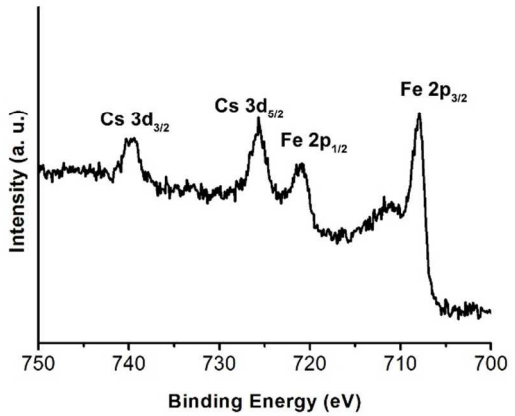


**Fig. 2** XPS spectrum of Cs promoted $Fe_5C_2$/charcoal at Cs/Fe=0.025.

### 3.1. Synthesis of Cs promoted $Fe_5C_2$/charcoal catalysts

Scheme 1 demonstrates the overall synthetic procedure for the Cs promoted iron-carbide/charcoal nanocatalyst. The active iron-carbide nanoparticles doped by Cs were successfully embedded in the activated charcoal support using two simple processes, i.e., melt infiltration of the hydrated iron salt and wetness impregnation of the Cs solution with subsequent calcination. In the first step, the $Fe(NO_3)_3 \bullet 9H_2O$ salt was melt-infiltrated into mesoporous charcoal by grinding it at room temperature and subsequently aging the reaction mixture at 323 K for 24 h in an oven. Next, the amorphous iron salt in charcoal was transformed to tiny iron-carbide nanoparticles by thermal decomposition at 623 K under a CO flow. In the second step, iron-carbide nanoparticles supported on porous charcoal were doped with Cs by impregnating the aqueous $Cs_2CO_3$ solution and thermally treating it again at 623 K under CO flow. The Cs/Fe atomic ratios in the Cs promoted iron-carbide particles were controlled using different concentrations of aqueous $Cs_2CO_3$ solution.

The transmission electron microscopy (TEM) image shows the iron-carbide incorporated charcoal at an atomic ratio of Cs/Fe of 0.025 (**Fig. 1a**). The small iron-carbide nanoparticles were well-dispersed in the charcoal support; these nanoparticles were observed to be 8.5±1.4 nm in average particle size (**Fig. S1a-b, Supporting Information**). The high-angle annular dark-field scanning transmission electron microscopy (HAADF-STEM) image shows bright spots and relatively dark regions indicating iron-carbide nanoparticles and carbon support structures, respectively (**Fig. 1b**). High-resolution TEM (HRTEM) and corresponding Fourier-transform pattern analysis revealed that the final Cs promoted iron-carbide particle, with spherical shape, was a single crystal with a distance of 0.208 nm between neighboring fringes, well matched with the (021) planes of iron-carbide (**Fig. 1c**). The Cs promoted iron-carbide particles at a Cs/Fe ratio of 0.050 showed slightly irregular and enlarged particle size, which was measured and found to be 13.8±2.8 nm (**Fig. 1d**, **Fig. S1c-d**). The X-ray diffraction (XRD) spectra, with a broad peak at $2\theta$= 43-45°, show that the Cs promoted iron-carbide particles at ratios of both Cs/Fe=0.025 and Cs/Fe=0.050 are matched with two monoclinic Hägg-carbide($Fe_5C_2$) phases (**Fig. 1e**, JCPDS No. 36-1248 and No. 51-0997). In the XRD spectra, no significant peaks related to any crystalline cesium compounds were observed.

To check the surface state of the Cs promoted $Fe_5C_2$ particles, the core-level X-ray photoelectron spectroscopy (XPS)

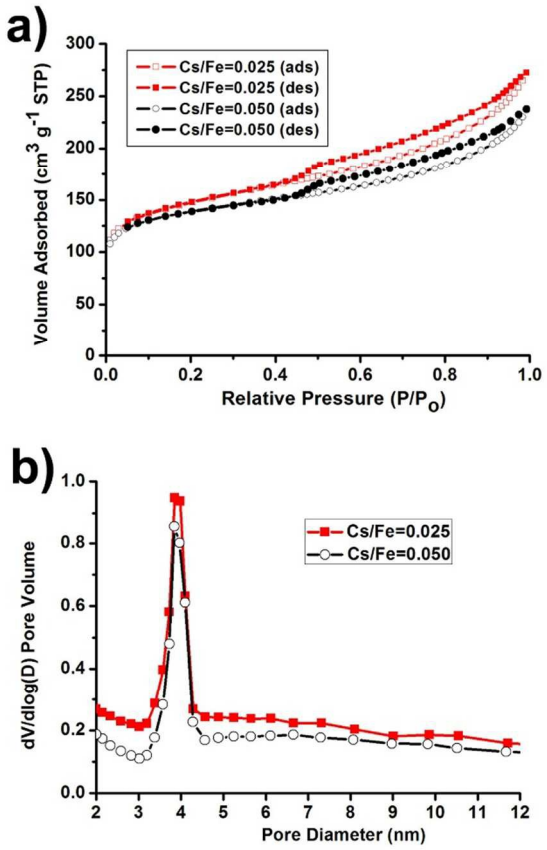


**Fig. 3** (a) $N_2$ adsorption/desorption isotherms and (b) pore size distribution diagrams of Cs promoted $Fe_5C_2$ on charcoal catalysts.

spectrum of Fe and Cs were measured. The XPS spectra of the energy regions of the Cs and Fe bands exhibit two sets of assigned sharp peaks: from iron carbide (Fe(0)) at 707.9 eV and 721.0 eV, and from cesium (Cs(0)) at 725.7 and 739.5 eV (**Fig. 2**). Another weak peak at 710.8 eV shows that the iron oxide phase (Fe(3+)) originated from the slightly oxidized surfaces of the $Fe_5C_2$ during the sampling process.

All Fe-loading contents in the Cs promoted $Fe_5C_2$/charcoal catalysts were calculated and found to be approximately 20wt% on the basis of Fe converted from iron nitrate salt after thermal decomposition. The Cs content in the total catalyst weight, which is the sum of $Fe_5C_2$, Cs, and the charcoal, was calculated and found to be ca. 1wt% at Cs/Fe=0.025 and 2wt% at Cs/Fe=0.050 on the basis of Cs converted from the cesium carbonate precursor. $N_2$ sorption experiments at 77 K for the Cs promoted $Fe_5C_2$/charcoal catalysts exhibited type IV adsorption-desorption hysteresis with delayed capillary evaporation at a relative pressure of 0.5 (**Fig. 3a**). The Brunauer-Emmett-Teller (BET) surface areas of the Cs promoted $Fe_5C_2$/charcoal were calculated and found to be 541.1 $m^2 \bullet g^{-1}$ at Cs/Fe=0.025 and 516.2 $m^2 \bullet g^{-1}$ at Cs/Fe=0.050. The total pore volumes were also measured to be 0.42 $cm^3 \bullet g^{-1}$ at Cs/Fe=0.025 and 0.37 $cm^3 \bullet g^{-1}$ at Cs/Fe=0.050. The slightly decreased BET surface area and pore volume at Cs/Fe=0.050 can be mainly attributed to the enlarged $Fe_5C_2$ particle size of 13.8 nm, which is larger than that of Cs/Fe=0.025 (8.5 nm). Using the Barrett-Joyner-Halenda (BJH) method on the desorption branches, the small pore sizes of Cs promoted

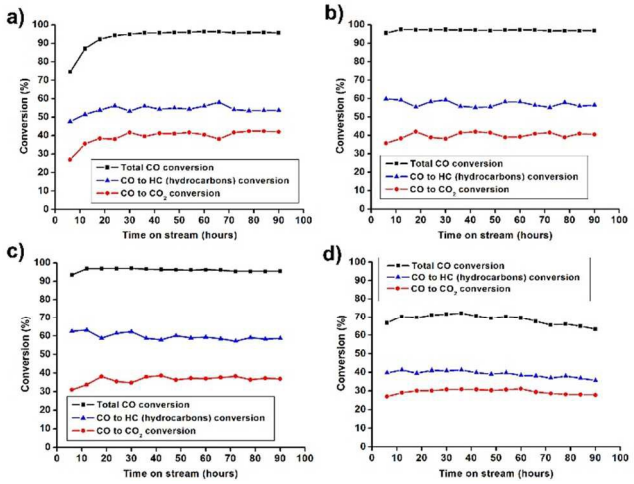


**Fig. 4** CO conversion graphs of Cs promoted $Fe_5C_2$/charcoal catalysts at (a) Cs/Fe = 0.010, (b) Cs/Fe = 0.025, (c) Cs/Fe = 0.050, and (d) Cs/Fe = 0.100. The total CO conversion is the sum of the the CO conversion to hydrocarbons (CO to HC) and the CO conversion to $CO_2$ (CO to $CO_2$). The reaction tests were conducted at 320 °C, 15 bar, and a $H_2$:CO ratio of 1.

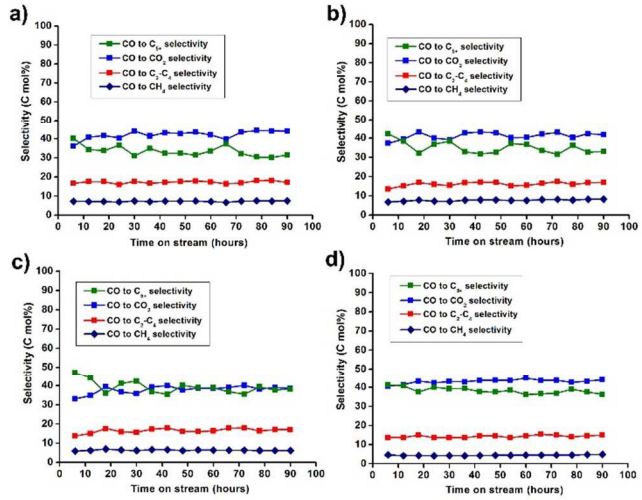


**Fig. 5** $CO_2$ and hydrocarbon product selectivity graphs for Cs promoted $Fe_5C_2$/charcoal catalysts at (a) Cs/Fe = 0.010, (b) Cs/Fe = 0.025, (c) Cs/Fe = 0.050, and (d) Cs/Fe = 0.100.

$Fe_5C_2$/charcoal catalysts were found to be equal at 3.8 nm (**Fig. 3b**).

To verify the basicity change on Cs promoted catalysts, the amount of $CO_2$ uptake, which can reflect the intensity of the surface basicity, was measured by temperature-programmed desorption (TPD) using $CO_2$. In the previous results, alkali metals such as Na and K played a crucial role in enhancing the surface basicity of iron-based catalysts because the alkali promoters strongly donate the single electron in their s-orbital to the d-orbital of iron.[36-38] As expected, the more Cs promoted catalyst at Cs/Fe=0.025 showed higher basicity with intensive peaks at higher temperatures of 250-300 °C than those of the Cs-poor catalyst at Cs/Fe=0.010. The $CO_2$ desorption amount was measured to be 0.291 mmol•$g^{-1}$ at Cs/Fe=0.010 and 0.446 mmol•$g^{-1}$ at Cs/Fe=0.025 (**Fig. S2**). The strong peaks above 250 °C are ascribed to the strong adsorption of $CO_2$ interacted with the surface basic site. At Cs/Fe=0.050, the amount of $CO_2$ desorption was obtained to be 0.493 mmol•$g^{-1}$ which is larger than those of Cs/Fe=0.010~0.025.

### 3.2. High-temperature Fischer-Tropsch Synthesis reaction

High-temperature FT synthesis was carried out at 15 bar, 320°C, and an $H_2$/CO ratio of 1. The CO conversion and selectivity of the Cs promoted $Fe_5C_2$ catalysts were measured for 90 h on a stream of a reaction; results were obtained by gas chromatography (GC) analysis of the outlet gasses containing the unreacted CO, $H_2$, $CH_4$, $C_2$–$C_4$ hydrocarbons, and $CO_2$. Liquid hydrocarbons obtained in a cold trap and solid hydrocarbons obtained in a hot trap were analysed by simulated distillation (SIMDIS). The hydrocarbon formation proceeds by FT synthesis as follows:

$$nCO + (2n+1)H_2 \rightarrow CnH_{2n+2} + nH_2O : \text{paraffins}$$

$$nCO + 2nH_2 \rightarrow CnH_{2n} + nH_2O : \text{olefins}$$

$CO_2$ could be also generated by the accompanied WGS reaction as follows:

$$CO + H_2O \leftrightarrow CO_2 + H_2$$

Cs promoted $Fe_5C_2$/charcoal catalysts at Cs/Fe=0.025 and Cs/Fe=0.050 showed very high total CO conversions of 96.9% and 95.5% without deactivation. Moreover, the CO conversion quickly reached a steady-state within 12 h of reaction (**Fig. 4b-c**). But, the $Fe_5C_2$/charcoal catalyst at Cs/Fe=0.010 exhibited lower CO conversion with longer induction period (~30 h) during FT reaction (**Fig. 4a**). The promoter-free $Fe_5C_2$ catalyst have also showed a similar trend with long induction period (~66 h) in our previous result.[32] Although Cs is a very strong base promoter, which easily donate electrons to active iron carbide surfaces, the more Cs doped catalyst than Cs/Fe=0.010 is needed to maximize its effect. The conversion rates of CO to HC and CO to $CO_2$ for a time-on-stream (TOS) of 90 h were observed to be 56.4% and 40.5% at Cs/Fe=0.025 (**Fig. 4b**) and 58.7% and 36.8% at Cs/Fe=0.050 (**Fig. 4c**), respectively.

In the selectivity data, the graph of Cs/Fe=0.025 shows the selectivity of $CH_4$ (8.3%), $C_2$-$C_4$ (16.9%), and $C_{5+}$ (33.1%) at TOS 90 h (**Fig. 5b**). On the other hand, at Cs/Fe=0.050, lower $CH_4$ selectivity (6.2%) and higher $C_{5+}$ selectivity (38.2%) were obtained (**Fig. 5c**). The higher selectivity for heavy hydrocarbons at Cs/Fe=0.050 can be mainly attributed to the higher surface basicity of the catalyst, as has been reported elsewhere.[39] The surface basicity, which was controlled by the Cs/Fe atomic ratio, affected the dissociative adsorption of CO and the adsorption of $H_2$, leading to a modification of the selectivity for the target hydrocarbon products. However, under the excess Cs promoted $Fe_5C_2$ catalyst at Cs/Fe=0.1, much lower CO conversion (63.3%) and higher $CO_2$ selectivity (43.9%) than those of Cs/Fe=0.05 were observed (**Fig. 4d, Fig. 5d**). We believe that the low CO conversion and gradual deactivation at Cs/Fe=0.100 after 54 h reaction are mainly attributed to the relatively poor CO dissociation property compared to its CO adsorption property.[32]

The catalytic activity was noted as iron-time-yield (FTY, i.e., the number of CO moles converted to hydrocarbons per gram of iron per second), which reflects the CO conversion and

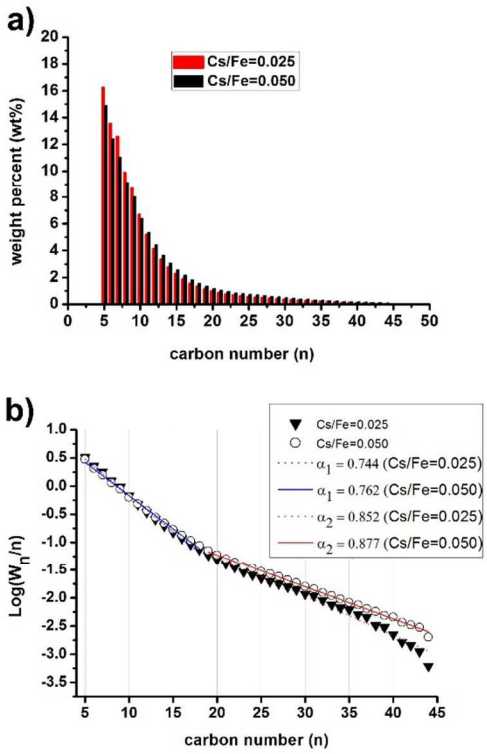


**Fig. 6** (a) Hydrocarbon product distribution and (b) ASF plots of $C_{5+}$ hydrocarbons and chain growth probability.

hydrocarbon selectivity of the catalyst during the FT reaction (**Fig. S3**). The Cs promoted $Fe_5C_2$ catalyst at Cs/Fe=0.050 showed a slightly higher FTY value of $1.454\times10^{-4}$ $mol_{CO}\bullet g_{Fe}^{-1}\bullet s^{-1}$ than that of the Cs/Fe=0.025 ($1.398\times10^{-4}$ $mol_{CO}\bullet g_{Fe}^{-1}\bullet s^{-1}$) due to its lower CO to $CO_2$ selectivity (38.6%) than 40.4% at Cs/Fe=0.025. The FT activities of the Cs promoted catalysts at both Cs/Fe=0.025 and Cs/Fe=0.050 were very high, compared to those of the previously reported values on supported iron catalysts reacted under high temperature conditions (**Table S1**). Interestingly, the Cs promoted $Fe_5C_2$ catalyst at Cs/Fe=0.025 showed very high liquid oil productivity of 0.401 $g_{liq}\bullet g_{cat}^{-1}\bullet h^{-1}$ after the FT reaction for 90 h, compared to that of Cs/Fe=0.050 (0.296 $g_{liq}\bullet g_{cat}^{-1}\bullet h^{-1}$) (**Table S2**). On the contrary, the solid wax productivity of Cs/Fe=0.025 was very low, compared to the high liquid oil productivity, observed to be 0.026 $g_{sol}\bullet g_{cat}^{-1}\bullet h^{-1}$ which is a much lower value than that obtained using Cs/Fe=0.050 (0.164 $g_{sol}\bullet g_{cat}^{-1}\bullet h^{-1}$). The detailed composition of the liquid and solid hydrocarbons was analysed by ASTM D2887 (**Fig. 6a**). The chain growth probability ($\alpha$) of the hydrocarbons was calculated using the Anderson-Schulz-Flory (ASF) chain growth mechanism in the following equation,[40] in which $W_n$ is the weight fraction of hydrocarbons with carbon number n (**Fig. 6b**):

$$\log(W_n/n) = \log(\ln^2\alpha) + n\bullet\log\alpha$$

Two $\alpha$ values ($\alpha_1$ from $C_5$ to $C_{18}$ and $\alpha_2$ from $C_{19}$ and $C_{44}$) were obtained by the slope of the graph which is fitted by two linear regressions. Low $\alpha$ values of 0.744 at Cs/Fe=0.025 and 0.762 at Cs/Fe=0.050 and high $\alpha$ values of 0.852 at Cs/Fe=0.025 and 0.877 at Cs/Fe=0.050 are attributed to Cs-lean sites and Cs-rich sites of the catalysts, respectively. The $\alpha$ values ($\alpha_1 = 0.762$ and $\alpha_2 = 0.877$) at Cs/Fe=0.050 were higher than those calcuated at Cs/Fe=0.025, demonstrating that a larger Cs doped $Fe_5C_2$ surface can provide more advantageous conditions for the growth of carbon chains during FT synthesis.

For the gaseous hydrocarbon products ($C_1$-$C_4$ gasses), the hydrocarbon product yields (grams of generated hydrocarbons per gram of iron per second) were calculated (**Table S3**). For the Cs promoted $Fe_5C_2$ catalyst at Cs/Fe=0.025, the total gas product yield was relatively high ($8.56\times10^{-4}$ $g_{HC}\bullet g_{Fe}^{-1}\bullet s^{-1}$) compared to that obtained at Cs/Fe=0.050 ($8.03\times10^{-4}$ $g_{HC}\bullet g_{Fe}^{-1}\bullet s^{-1}$). But, the product yield ratio of $C_2$-$C_4$ olefins to $C_2$-$C_4$ praffins at Cs/Fe=0.025 was much lower (0.53) than that of Cs/Fe=0.050 (1.82). In total weight portions of $CH_4$, $C_2$-$C_4$ olefins, $C_2$-$C_4$ paraffins, $C_5$-$C_{12}$, $C_{13}$-$C_{18}$, and $C_{19+}$ of the Cs promoted $Fe_5C_2$ catalysts, heavy hydrocarbon portion ($C_{19+}$) was significantly low at Cs/Fe=0.025, because of the relatively low surface basicity of the catalyst (**Fig. S4**). Therefore, in high-temperature FT synthesis, because such a combination can increase the CO conversion rate and decrease the solid wax formation, a combination of proper reaction temperature (320 $^oC$) and reaction pressure (15 bar), and use of Cs promoted Fe catalyst at Cs/Fe=0.025 could be the best method for the selective production of liquid oil at high productivity. After the reactions, the Cs promoted catalysts showed slightly increased $Fe_5C_2$ particles in size which reflect the separated peaks in the XRD data, but still maintained their original structures without the severe particle aggregation (**Fig S5**).

## Conclusions

Cs promoted $Fe_5C_2$/charcoal nanocatalysts with a controlled Cs/Fe atomic ratio were simply prepared via a facile melt-infiltration process and incipient wetness method. The catalyst at Cs/Fe=0.025, based on the small $Fe_5C_2$ particle size (8.5 nm) and surface basicity promoted by appropriate Cs doping, showed very high CO conversion (>95%) and liquid oil productivity (~0.4 $g_{liq}\bullet g_{cat}^{-1}\bullet h^{-1}$) in high-temperature FT synthesis. Furthermore, it is anticipated that the Cs promoted $Fe_5C_2$/charcoal nanocatalysts will serve as commercially applicable catalyst platforms that will lead to the sustainable production of liquid oil in high-temperature FT synthesis.

## Acknowledgements

This work was conducted under the National Research and Development Program of the Korea Institute of Energy Technology Evaluation and Planning (NP-2012-0020/B4-3207). The authors greatly appreciate the technical support of Mr. Seong Bum Yoo (Hanbat National University, Republic of Korea).

## Notes and references

[a] Clean Fuel Laboratory, Korea Institute of Energy Research, 152 Gajeong-Ro, Daejeon, 305-343, Korea. Tel: 82-42-860-3605; E-mail: jcpark@kier.re.kr, jungh@kier.re.kr

[b] Advanced Energy and Technology, University of Science and Technology, 217 Gajeong-Ro, Daejeon, 305-343, Korea.

Electronic Supplementary Information (ESI) available: TEM images and particle size distribution histograms, $CO_2$ TPD profiles, FTY graphs, hydrocarbon distribution (weight percent) data, TEM and XRD data of the recovered catalysts, hydrocarbon productivity, and gas product yields of Cs promoted $Fe_5C_2$ nanocatalysts. See DOI: 10.1039/c000000x/

1 M. E. dry, *Catal. Today* 2002, **71**, 227.
2 H. Schulz, *Appl. Catal. A: Gen.* 1999, **186**, 3.
3 Q. Zhang, J. Kang and Y. Wang, *ChemCatChem* 2010, **2**, 1030.
4 R. Luque, A. R. de la Osa, J. M. Campelo, A. A. Romero, J. L. Valverde and P. Sanchez, *Energy Environ. Sci.* 2012, **5**, 5186.
5 E. de Smit and B. M. Weckhuysen, *Chem. Soc. Rev.* 2008, **37**, 2758.
6 O. O. James, B. Chowdhury, M. A. Mesubi and S. Maity, *RSC Adv.* 2012, **2**, 7347.
7 H. M. T. Galvis, J. H. Bitter, C. B. Khare, M. Ruitenbeek, A. I. Dugulan and K. P. de Jong, *Science*, 2012, **335**, 835.
8 H. M. T. Galvis and K. P. de jong, *ACS Catal.* 2013, **3**, 2130.
9 H. M. T. Galvis, J. H. Bitter, T. Davidian, M. Ruitenbeek, A. I. Dugulan and K. P. de Jong, *J. Am. Chem. Soc.* 2012, **134**, 16207.
10 C. Kibby, K. Jothimurugesan, T. Das, H. S. Lacheen, T. Rea and R. J. Saxton, *Catal. Today* 2013, **215**, 131.
11 X. Li, J. He, M. Meng, Y. Yoneyama and N. Tsubaki, *J. Catal.* 2009, **265**, 26.
12 J. Kang, K. Cheng, L, Zhang, Q. Zhang, J. Ding, W. Hua, Y. Lou, Q. Zhai and Y. Wang, *Angew. Chem. Int. Ed.* 2011, **50**, 5200.
13 A. V. Karre, A. Kababji, E. L. Kugler and D. B. Dadyburjor, *Catal. Today* 2012, **198**, 280.
14 S.-H. Kang, J. W. Bae, P. S. S. Prasad and K.-W. Jun, *Catal. Lett.* 2008, **125**, 264.
15 J.-C. Kim, S. Lee, K. Cho, K. Na, C. Lee and R. Ryoo, *ACS Catal.* 2014, **4**, 3919.
16 C. Ngamcharcharussrivichai, A. Imyim, X. Li and K. Fujimoto, *Ind. Eng. Chem. Res.* 2007, **46**, 6883.
17 A. de Klerk, *Green Chem.* 2008, **10**, 1249.
18 E. van Steen and M. Claeys, *Chem. Eng. Technol.* 2008, **31**, 655.
19 D. Leckel, *Energy Fuels* 2009, **23**, 2342.
20 T. Herranz, S. Rojas, F. J. Pérez-Alonso, M. Ojeda, P. Terreros and J. L. G. Fierro, *J. Catal.* 2006, **243**, 199.
21 V. R. R. Pendyala, G. Jacobs, H. H. Hamdeh, W. D. Shafer, D. E. Sparks, S. Hopps and B. H. Davis, *Catal. Lett.* 2014, **144**, 1624.
22 E. de Smit, F. Cinquini, A. M. Beale, O. V. Safonova, W. van Beek, P. Sautet and B. M. Weckhuysen, *J. Am. Chem. Soc.* 2010, **132**, 14928.
23 C. Yang, H. Zhao, Y. Hou and D. Ma, *J. Am. Chem. Soc.* 2012, **134**, 15814.
24 A. Meffre, B. Mehdaoui, B. Kelsen, P. F. Fazzini, J. Carrey, S. Lachaize, M. Respaud and B. Chaudret, *Nano. Lett.* 2012, **12**, 4722.
25 T. M. Eggenhuisen, J. P. den Breejen, D. Verdoes, P. E. de Jongh and K. P. de Jong, *J. Am. Chem. Soc.* 2010, **132**, 18318.
26 H. Woo, K. Lee, J. C. Park and K. H. Park, *New J. Chem.* 2014, **38**, 5626.
27 P. E. de Jongh, R. W. P. Wagemans, T. M. Eggenhuisen, B. S. Dauvillier, P. B. Radstake, J. D. Meeldijk, J. W. Geus and K. P. de Jong, *Chem. Mater.* 2007, **19**, 6052.
28 W. Ngantsoue-Hoc, Y. Zhang, R. J. O'Brien, M. Luo and B. H. Davis *Appl. Catal. A: Gen.* 2002, **236**, 77.
29 M, Luo and B. H. Davis, *Appl. Catal. A: Gen.* 2003, **246**, 171.
30 A. N. Pour, S. M. K. Shahri, H. R. Bozogzadeh, Y. Zamani, A. Tavasoli and M. A. Marvast, *App. Catal. A. Gen.* 2008, **348**, 201.
31 D. C. Sorescu, *Surf. Sci.* 2011, **605**, 401.
32 J. C. Park, S. C. Yeo, D. H. Chun, J. T. Lim, J.-I. Yang, H.-T. Lee, S. Hong, H. M. Lee, C. S. Kim and H. Jung, *J. Mater. Chem. A* 2014, **2**, 14371.
33 K. N. Rao and H. P. Ha, *Catal. Sci. Technol.* 2012, **2**, 495.
34 J. Gaube and H.-F. Klein, *Appl. Catal. A: Gen.* 2008, **350**, 216.
35 E. van Steen and F. F. Prinsloo, *Catal. Today* 2002, **71**, 327.
36 W. Hou, B. Wu, X. An, T. Li, Z. Tao, H. Zheng, H. Xiang and Y. Li, *Catal. Lett.* 2007, **119**, 353.
37 X. An, B.-S. Wu, H.-J. Wan, T.-Z. Li, Z.-C. Tao, H.-W. Xiang and Y.-W. Li, *Catal. Commun.* 2007, **8**, 1957.
38 G. Zhao, C. Zhang, S. Qin, H. Xiang and Y. Li, *J. Mol. Catal. A-Chem.* 2008, **286**, 137.
39 M. E. Dry and G. J. Oosthuizen, *J. Catal.* 1968, **11**, 18.
40 I. Puskas and R. S. Hurlbut, *Catal. Today* 2003, **84**, 99.



 

# Graphical Abstract

Cs promoted $Fe_5C_2$/charcoal nanocatalysts bearing small iron carbide particles were prepared using a simple melt-infiltration process for high-temperature Fischer-Trospch reaction. Due to the optimized basicity by Cs, the catalyst at Cs/Fe=0.025 demonstrated excellent catalytic performance in liquid fuel production.